Characterization of Some EPDM-g-MA/OMMT Nanocomposites

DANIELA MARIA STELESCU[1]*, ANTON AIRINEI[2], MIHAELA HOMOCIANU[2], DANIEL TIMPU[2], CRISTIAN GRIGORAS[2]

[1]National Research and Development Institute for Textile, Leather, and Footwear Research, 93 Ion Minulescu Str., 031215, Bucharest, Romania

[2]"Petru Poni" Institute of Macromolecular Chemistry, 41A Aleea Grigore Ghica Voda, 700487, Iasi, Romania

(Nano)composites based on maleated ethylene propylene diene terpolymer (EPDM-g-AM) and organically modified montmorillonite (OMMT) has been prepared by melt intercalation procedure. The materials were characterized by X-ray diffraction (XRD), thermogravimetric analysis (TGA), dynamic scanning calorimetry (DSC) and mechanical tests. XRD data show the increase of the distance between the silicate layers indicating the intercalation of polymer chains in the montmorillonite galleries. The incorporation of OMMT in composites determines the increase of melting peak temperature (T_m) and heat of fusion (ΔH_f) suggesting a supplementary nucleation increase due to the OMMT presence. The mechanical properties were analyzed as a function of the OMMT level in the composite and the results reveal remarkable improvement relative to the conventional composite.

Keywords: EPDM-g-MA/OMMT nanocomposites, XRD, TGA, DSC, mechanical properties

In the last decades, polymer/layered clay nanocomposites (PCN) have attracted considerable attention in both basic research and industry exploitation because they possess a combination of properties that are not available in any of the single components. These systems exhibited improvements in mechanical properties, thermal stability, gas barrier properties, flame retardance, chemical and dimension stability [1-11]. All these benefits are obtained at low loading levels of nanofiller (less than 5% by weight) [11].

The most commonly used clay to obtain PCN is montmorillonite and it can undergo intercalation with organic molecules. In order to improve the affinity between hydrophilic layered silicate and the hydrophobic polymer the replacement of the exchange cations in the galleries of the clay through organic cations such as alkyl ammonium ions to form organo-silicates was performed [6, 11, 12].

When the organomodified clay particles are dispersed in the polymer matrix three different types of structures can be found in nanocomposites: intercalated, flocculated and exfoliated. In the intercalated structures the polymer chains have penetrated into the layered structure maintaining the well-order multilayered nature. The flocculated structure is similar to the intercalated one, but the intercalated silicate layers sometimes flocculated because of the hydroxylated edge-edge interactions. The exfoliated structures of the silicate nanolayers are randomly dispersed throughout the polymer matrix. The exfoliated structures will determine enhanced properties of nanocomposites due to their higher phase homogeneity as compared to intercalated ones [6, 13, 14]. XRD at small angles ($2\theta < 10^o$) is an effective method to study these structures present in nanocomposites beside transmission electron microscopy (TEM). XRD data exhibit some peaks whose position is related to the basal spacing d_{001} and its broadness can give information about the distribution of spacings. In the exfoliated structures the interlayer spacing can be of the order of the gyration radius of the polymer and no peaks in their region are present due to the large d-spacings (10 nm) [6, 15]. Transmission electron microscopy gives the possibility to obtain data on the delaminated layers or intercalated stacks. The intercalation/exfoliation of layered clays is determined by compatibility of components, polymer diffusivity and processing conditions.

Exfoliation process is facilitated by the addition of polymers containing functional groups, mainly polypropylene grafted with maleic anhydride (PP-g-MA), as a compatibilizer to improve the dispersion of clay and mechanical properties of the nanocomposites [16-19].

PCN can be fabricated by different methods, such as solution intercalation, in-situ intercalation polymerization and polymer melt intercalation. The melt compounding method is more advantageous due to its compatibility with current industrial polymer processing procedures and its environmental benefit determined by the lack of solvents [18, 20, 21]. The properties of nanocomposites obtained by melt blending technique can be controlled by various parameters: molecular architecture of the alkylammonium cation used in ionic exchange, the presence of additives during silicate modification, processing temperature, the type and the content of compatibilizer and polymer viscosity [21, 22].

In this work the preparation of some EPDM-g-MA/OMMT nanocomposites using melt blending was described. The dispersability of organoclay in the EPDM-g-AM matrix has been estimated by X-ray diffractometry. Mechanical and thermal properties have been also studied.

Experimental part

Materials

EPDM-g-MA Royaltuf 498 with a graft percentage of 1.0 % and Mooney viscosity of 30 M2(1+4) at 125°C was used in the present work. The organoclay was montmorillonite intercalated by octadecyltrimethylamine with commercial name Nanomer 128E. The other compounding ingredients such as zinc oxide (neutralizing agent), stearic acid (processing aid), zinc stearate (ionic plasticizer), Irganox 1010 (antioxidant) were also used in recipe. PP-g-MA Polybond 3002 with 1% MA and melting flow index (MFI) of 7.0 g/10 min at 230°C/2.16 kg was utilized as compatibilizing agent.

* Tel.: 021 323 50 60

Equipment

X-ray diffractograms were collected from a Bruker A8 Advance diffractometer with Ni-filtered Cu-Kα radiation (λ = 0.1541 nm) operating a tube voltage of 40 kV and a tube current of 35 mA. The diffractograms were scanned in 2θ range from 1°-30° at a rate of 1 °/min. The interlayer spacing (d_{001}-spacing) was evaluated by the Braag equation: $\lambda = 2d \sin\theta$, where θ is the diffraction angle, λ is the x-ray wavelength and d is the interlayer spacing.

Tensile measuring test was carried out with a Schoppler strength tester, using dumb-bell shaped specimens according to ISO 37/1997. Hardness was measured by using a hardner tester according to ISO 7619/2001. Tear strength was performed according to ISO 34-1/2000 using angular test pieces (type II). Elasticity was evaluated with a test machine of type Schob. All measurements were taken several times and the result values were averaged.

Dynamic scanning calorimetry (DSC) measurements were performed on Perkin Elmer Pyris Diamond calorimeter, at a heating rate of 15°C/min. Thermogravimetric analysis (TGA) was conducted on MOM Derivatograpgh at a heating rate of 10°C/min. The samples were heated in the temperature range from room to 750°C in air.

Preparation of (nano)composites

Three compositions containing EPDM-g-MA were prepared according to table 1.

Table 1
EPDM-g-MA COMPOSITIONS

Code	Compound
1 - MA0	EPDM-g-MA
2 - MA	EPDM-g-MA/OMMT
3 - PMA	EPDM-g-MA/OMMT/PP-g-MA

The above-mentioned compositions were prepared through melt blending method. The compositions **1** and **2** were obtained using a Plasti-Corder Brabbender PLV330 equipment at 100 rpm, at a temperature of 170°C for 12 min as blending time. The composition **3** was performed with a Plasti-Corder Brabender PLV330 equipment at 100 rpm, at a temperature of 190°C for 12 min, with a PP-g-MA/clay ratio of 3:1. The compositions contain also compounding ingredients such as zinc oxide (10 g), stearic acid (1 g), zinc stearate (20 g) and Irganox 1010 (2 g). The resultant composites were homogenized on an electrically operated laboratory roller mill at 155-165°C. The test specimens for physico-mechanical measurements were obtained by pressing in an electrical press at 170°C for 5 min and pressure of 150 MPa.

Results and discussion

The structure of nanocomposites was characterized by X-ray diffractometry. Figure 1 shows the diffraction patterns of OMMT, initial sample (MA0) and of two (nano) composites - for compositions **2** and **3** 100 g of EPDM-g-MA, 7.5 g of OMMT and 22.5 g of PP-g-MA, respectively were used. The modified organoclay shows two 2θ peaks at 3.81° and 5.65 ° which correspond to a basal spacing of 2.32 and 1.56 nm, respectively (table 2). For the nanocomposites **2** and **3** a high increase in d-spacing of the layered silicate was observed (table 2) and the corresponding diffraction peak is shifted to lower 2θ angles namely 2.24°. The shift of the sharp diffraction peak of organoclay from 2θ = 3.81° to lower diffraction angles in our composites suggests that EPDM-g-MA has been able to intercalate into the gallery space of the layered silicate, expanding the basal spacing of organoclay which increases to 3.94 nm, which can clearly confirm the nanocomposite formation.

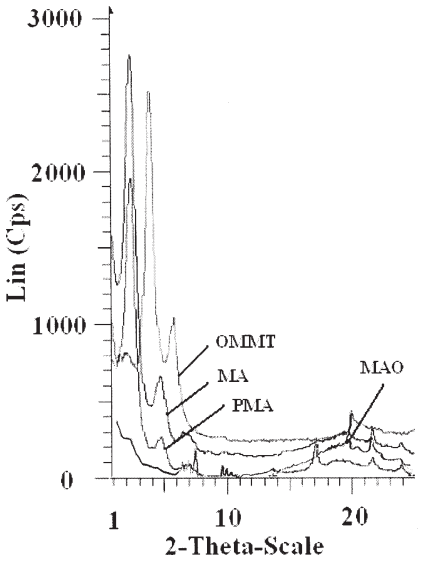

Fig. 1. XRD patterns of OMMT and EPDM-g-AM (nano)composites

The basal spacing increase in nanocomposites can be also determined by the presence of hydrogen bondings between the maleic anhydride groups and the oxygen of silicate. The greater polarity of the EPDM-g-MA facilitates the interdiffusion of the polymer chains into the gallery spaces of the organoclay leading to a better dispersion of the nanoclay in polymer matrix. As given in figure 1, the EPDM-g-MA/PP-g-MA nanocomposite **3** exhibits a diffraction peak at the same 2θ with the same basal spacing relating to sample MA (table 2).

It can be observed that the intensity of 2θ diffractive peak at 2.24° is practically the same for nanocomposites **2** and **3**, a slight decrease was found out for the peak at about 4.72° for the composition containing compatibilizer PP-g-MA. The X-ray diffractogram of MAO sample shows a wide diffraction maximum centered at 2 θ ° due to amorphous phase.

Table 2
DIFFRACTION PATTERN CHARACTERISTICS OF COMPOSITES

Sample	2θ (°)	d (nm)
OMMT	3.81	2.32
	5.65	1.56
	19.86	0.45
	26.74	0.33
MA	2.24	3.94
	4.61	1,92
	21.55	0.41
	23.82	0.37
PMA	2.24	3.94
	4.72	1.87
	17.02	0.52
	21.53	0.41

For the studied composites a diffraction peak appeared at around $2\theta = 6.54^{o}$. This peak at small diffraction angles can be determined by the presence in composites of some diffraction centers formed by the aggregation tendency of ionic species leading to the formation of some microphases enriched in ions within polymer matrix and it can be attributed to interaggregated interface, the distances between ionic aggregates being Braag spaces while other authors assigned this peak to intraaggregated phase [23-25].

The evolution of the weight loss of above-mentioned samples with temperature is depicted in figure 2. The modified organoclay exhibits two stage of decomposition, the first corresponds to the elimination of absorbed free and interlayer water. In the second stage the degradation of organic material occurs starting at 220°C. The temperature at which the weight loss was 5% can be considered the initial decomposition temperature (T_d).

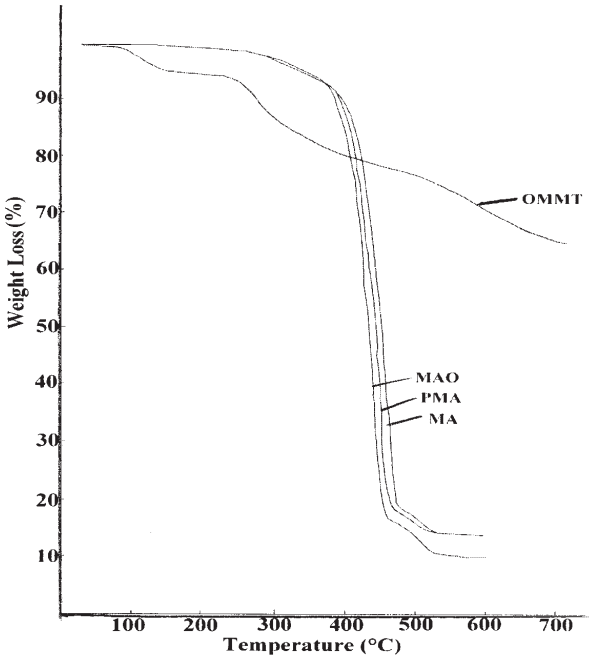

Fig. 2. TGA curves of OMMT and EPDM-g-AM (nano)composites

Table 3 summarized the thermal analysis data such as temperature at 5% weight loss, decomposition temperature at maximum weight loss rate (T_{max}), weight loss determined at the end decomposition (R). The three composites exhibit a very sharp weight loss of about 83% between 250 and 490°C, followed by a second short stage with maximum temperature near 510-530°C. As it can be noticed, the thermal stability of compositions containing nanoclay and compatibilizer was increased slightly compared to initial sample MAO. Also, the char residue has higher values in the first two compositions (MA and PMA). The thermal stability of EPDM-g-MA composites did not enhance as much, compared to the simple sample MAO. This small increase in thermal stability can be attributed to the clay nanolayers which can proceed as barriers to reduce the permeability of volatile degradation products from polymer matrix [26, 27]. From table 3 it can be seen that the organoclay practically does not decompose during processing or characterization of these materials.

DSC determinations were utilized to characterize melting and crystallization behaviour of composites based on EPDM-g-MA. Figures 3 and 4 depict the DSC cooling and reheating melt thermograms of composites under study. Some of representative data from DSC scans are presented in table 3 such as melting peak temperature (Tm), heat of fusion (ΔH_f), crystallization temperature (T_c). The melting process of EPDM-g-AM (nano)composites shows a broad endotherm peak between 65 and 130°C (fig. 3).

The melting temperatures for the first stage were found to be almost the same for all samples. The small decrease of melting temperature with the introduction of PP-g-MA as well as the decrease of exothermic signal intensities can be due to the decrease of maleated polypropylene crystallization in composition in the presence of EPDM-g-MA. Therefore PP-gAM retards the crystallization of PP. More than the incorporation of OMMT in composite (sample MA) determines the increase of T_m and of the fusion heat (table 3) suggesting a supplementary nucleation increase due to the nanoclay presence.

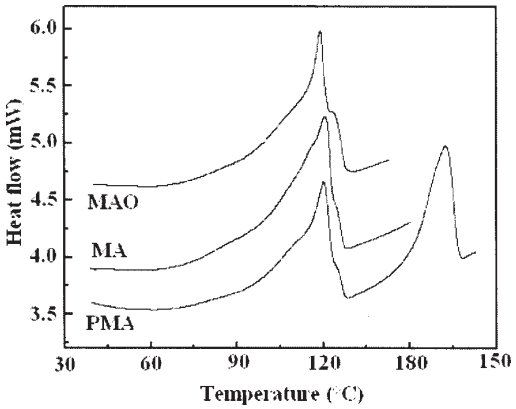

Fig. 3. DSC thermograms of samples

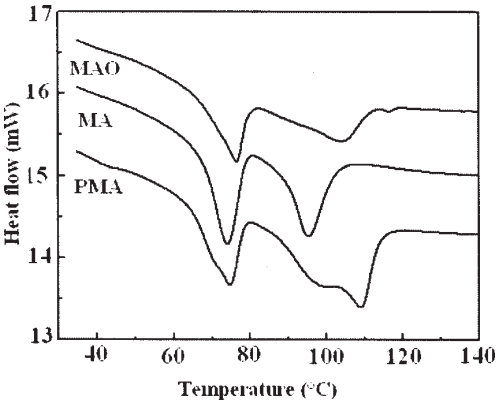

Fig. 4. DSC crystallization properties of samples

The crystallization temperature of PP-g-MA was around 118°C and this signed is shifted to 109°C after addition of OMMT and EPDM-g-MA in composition due to the limitation of chain mobility determined by the formation of hydrogen bonds between maleated EPDM and OMMT.

The mechanical properties of EPDM-g-MA (nano) composites under different OMMT loadings are presented in figures 5-10. Significant improvement in hardness, tensile strength, modulus and tear strength is clearly noticed for PMA nanocomposites containing compatibilizer with the increasing of OMMT content. Only the elasticity decreases with the increase of OMMT level in composites (fig. 7). The modulus and tensile strength increase rapidly with the increase of nanoclay loading (figs. 6 and 8) compared to that of MA sample. The enhancement in modulus and tensile strength shows that a better dispersion of layered silicate in polymer matrix in the presence of PP-g-MA as compatibilizer occurs and that the properties of the resulting polymer blends are additive. The tensile strength and elongation at break reach a maximum at about 2.5 phr of OMMT and then decrease (figs. 8 and 9), taking into

Table 3
THERMAL CHARACTERISTICS OF COMPOSITES

Sample	$T_{5\%}$ (°C)	T_{max} (°C)	R (%)	T_m (°C)	ΔH_f (J/g)	T_c (°C)
MAO	350	475	10.08	119.01	20.57	76.41 103.87
MA	340	460	13.31	120.52	22.07	74.02 95.24
PMA	335	455	13.91	120.17 162.34	16.45 11.84	74.64 108.97
PP-g -AM				163.23	85.70	118.01

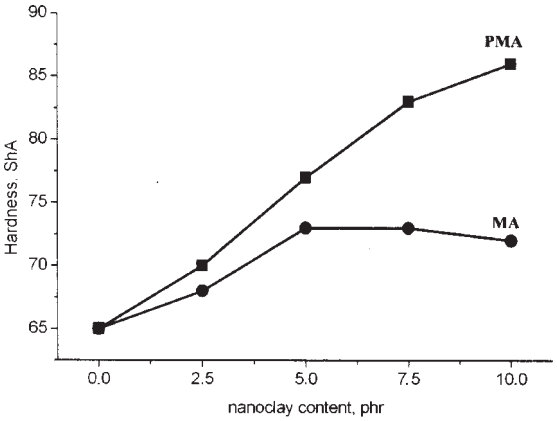

Fig. 5. Dependence of hardness on nanoclay content level

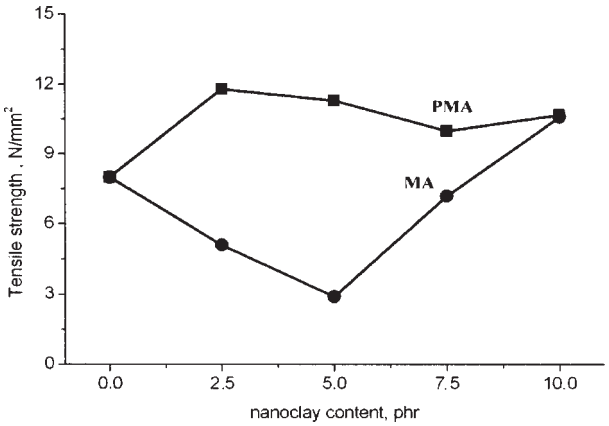

Fig. 8. Tensile strength as a function of nanoclay content

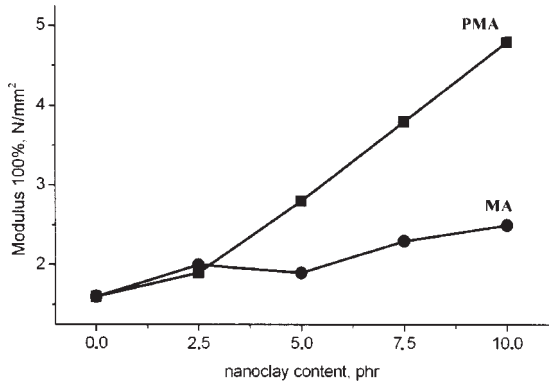

Fig. 6. Dependence of modulus 100% on nanoclay loading

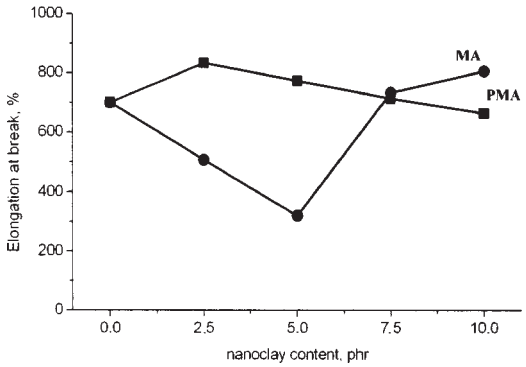

Fig. 9. Effect of nanoclay loading on elongation at break

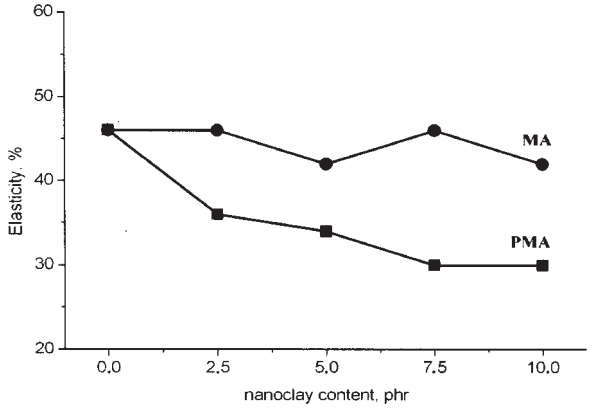

Fig. 7. Dependence of elasticity on nanoclay

account the aggregation of silicate layers in the case of high nanoclay level and the ability of EPDM-g-MA to accept high loadings of clay diminishes. However, tensile strength and elongation at break of the uncompatibilized sample (MA) show a minimum at 5 phr of OMMT content. This fact can be attributed to the decrease of ductibility while the stiffness become higher by reinforcing effect of OMMT layered silicate.

Tear strength and hardness exhibit a remarkable increase with increasing nanoclay level (figs. 5 and 10). This increase is due to the fact that the OMMT clay behaves as a reinforcing agent for the polymer matrix leading to the enhanced hardness.

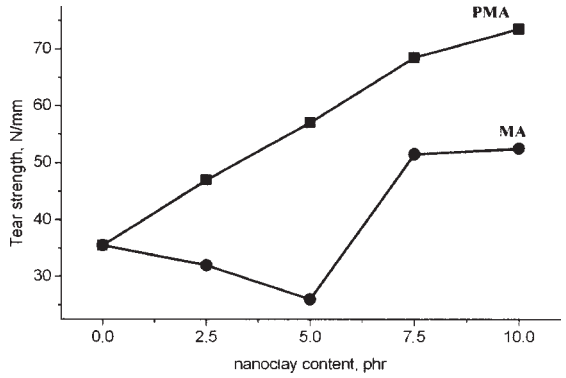

Fig. 10. Tear strength as a function of nanoclay content

Conclusions

(Nano)composites based on EPDM-g-MA and OMMT have been successfully obtained by melt intercalation procedure. XRD analysis indicated that the polymer chains can be intercalated intro the gallery space of OMMT because the distance between the silicate layers was increased, evidencing thus the formation of some EPDM-g-MA/OMMT nanocomposites. The thermal stability of compositions containing nanoclay and compatibilizer was increased slightly compared to initial sample MAO. The incorporation of OMMT in composites determines the increase of melting peak temperature (T_m) and heat of fusion (ΔH_f) suggesting a supplementary nucleation increase due to the OMMT presence. By increasing of OMMT content the hardness, modulus 100%, tear strength and tensile strength have increased, while elasticity and elongation at break have decreased for EPDM-g-MA/PP-g-MA/OMMT nanocomposites. These enhancements can be attributed to the reinforcing effect of layered silicate and to strong interactions between OMMT and polymer matrix in molten state.

References

1.PAVLIDOU, S., PAPASPYRIDES, C. D., Progr. Polym. Sci., **33**, 2009, p. 1119
2.BISWAS, M., RAY, S. S., Adv. Polym. Sci., **155**, 2009, p. 167
3.XU, R., MANIAS, E., SNYDER, A. J., RUNT, J., Macromolecules, **34**, 2001, p. 337
4.GILMAN, J. W., JACKSON, C. L., MORGAN, A. B., HARRIS, R., MANIAS, E., GRANNELLIS, E. P., WUTHENOW, M., HILTON, D., PHILLIPS, S. H., Chem. Mater., **12**, 2000, p. 1866
5. RAY, S. S., YAMADA, K., OKAMOTO, M., UEDA, K., Nano. Lett., **2**, 2002, p. 1093
6.KANG, D., KIM, D., YOON, S. H., KIM, D. BARRY, C., MEAD, J., Macromol. Mater. Eng., **292**, 2007, p. 329
7.PASBAKHSH, P., ISMAIL, H., FAUZI, M. N. A., BAKAR, A. A., Polym. Testing, **28**, 2009, p. 548
8.GALIMBERTI, M., SENATOSE, S., LOSTRITTO, A., GIANNINI, L., CONZATTI, L., COSTA, G., GUERRA, G., e-Polymers, No**. 057**, 2009, p. 1
9.FISHER, H., Mater. Eng. Sci., C **23**, 2003, p. 763
10.ACHARYA, H., KUILA, T., SRIVASTAVA, S. K., BHOWMICK, A. K., Polym. Compos., **29**, 2008, p. 443
11.RAY, S. S., OKAMOTO, M., Progr. Polym. Sci., **28**, 2003, p. 1539
12.AHMADI, S. J., HUANG, Y. D., LI, W. J., Compos. Mater., **39**, 2005, p. 745
13.RAY, S. S., OKAMOTO, K., OKAMOTO, M., Macromolecules, **36**, 2003, p. 2355
14.ROHLMANN, C. O., HORST, M. F., QUINZANI, L. M., FAILLA, M. D., Eur. Polym. J., **44**, 2008, p. 2749
15.COLE, K. C., Macromolecules, **41**, 2008, p. 834
16.KIM, K. N., KIM, H., LEE, W. J., Polym. Eng. Sci., **41**, 2009, p. 1963
17.KAEMPFER, D., THOMANN, R., MULHAUPT, R., Polymer, **43**, 2002, p. 2909
18.KAWASUMI, M., HASEGAWA, N., KATO, M., USUKI, A., OKADA, A., Macromolecules, **30**, 1997, p. 6333
19.SVOBODA, P., ZENG, C. C., WANG, H., LEE, L. J., TOMASKO, D. L., J. Appl. Polym. Sci., **85**, 2002, p. 1562
20.VAIA, R. A., GIANNELIS, E. P., Macromolecules, **30**, 1997, p. 7990
21.REICHERT, P., NIB, H., KLINKE, S., BRANDSCH, R., THOMAN, R., MULHAUPT, R., Macromol. Mater. Eng., **27**, 2000, p. 8
22.ABRANYI, A. A., SZAZDI, L., PUKANSZKY, B., Muanyag Gumi, **41**, 2004, p. 466
23. ZUGA, M.D., CINCU, C., Mat. Plast., **43,** no. 2, 2006, p. 90
24. ZUGA, M.D., CINCU, C., Mat. Plast., **43,** no. 3, 2006, p. 194
25. ANDREI, C., DOBRESCU V., Progrese în chimia şi tehnologia poliolefinelor, Ed. Ştiinţifică şi Enciclopedică, Bucureşti, **1987**
26. HSUEH, H. B., CHEN, C. Y., Polymer, **44**, 2003, p. 5275
27. AHMADI, S. J., HUANG, Y., LI, W., Compos. Sci. Technol., **65**, 2005, p. 1069

Manuscript received: 19.05.2010